

3-2016

Hydrothermal Single Crystal Growth and Characterization of Novel Rare Earth Niobates and Tantalates: LnNbO_4 (Ln = La-Lu, Y), $\text{La}_2\text{TaO}_5(\text{OH})$ and $\text{Ln}_3\text{Ta}_2\text{O}_9(\text{OH})$

Liurukara D. Sanjeewa
Clemson University

Kyle Fulle
Clemson University

Colin D. McMillen
Clemson University

Joseph W. Kolis
Clemson University

Follow this and additional works at: <https://tigerprints.clemson.edu/cars>

 Part of the [Chemistry Commons](#)

Recommended Citation

Sanjeewa, Liurukara D.; Fulle, Kyle; McMillen, Colin D.; and Kolis, Joseph W., "Hydrothermal Single Crystal Growth and Characterization of Novel Rare Earth Niobates and Tantalates: LnNbO_4 (Ln = La-Lu, Y), $\text{La}_2\text{TaO}_5(\text{OH})$ and $\text{Ln}_3\text{Ta}_2\text{O}_9(\text{OH})$ " (2016). *Chemistry Annual Research Symposium*. 1.
<https://tigerprints.clemson.edu/cars/1>

This Poster is brought to you for free and open access by the Student Works at TigerPrints. It has been accepted for inclusion in Chemistry Annual Research Symposium by an authorized administrator of TigerPrints. For more information, please contact kokeefe@clemson.edu.



Hydrothermal Single Crystal Growth and Characterization of Novel Rare Earth Niobates and Tantalates: LnNbO_4 ($\text{Ln} = \text{La-Lu, Y}$), $\text{La}_2\text{TaO}_5(\text{OH})$ and $\text{Ln}_3\text{Ta}_2\text{O}_9(\text{OH})$



Liurukara D. Sanjeeva¹, Kyle Fulle¹, Colin D. McMillen¹, Joseph W. Kolis^{1*}

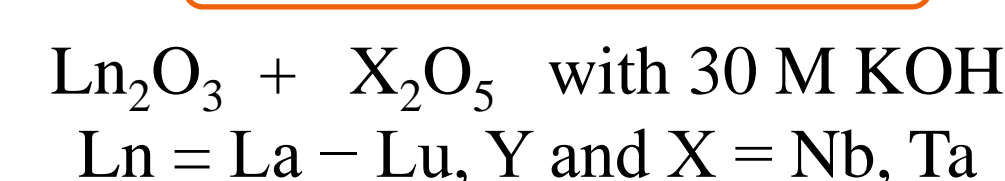
¹Department of Chemistry and Center for Optical Materials Science and Engineering Technologies (COMSET), Clemson University, Clemson, South Carolina 29634-0973, USA

Introduction

- Rare-earth niobates and tantalates are refractory materials that have been exploited in applications involving ion conductivity, photo-catalysis, and luminescence, both in doped and un-doped forms.
- In general, refractory oxides have high melting points therefore synthesis of single crystals are more challenging. For example LnNbO_4 can be grown readily by melt techniques such as Czochralski pulling $\sim 1300^\circ\text{C}$. However during the cooling crystal quality degraded resulting low quality crystals therefore high temperature melting techniques are not suitable for bulk single crystals growth.
- Development of alternative synthetic methods is one promising approach to realizing the full potential of the fundamental science and application of these materials.
- Of particular significance is the fact that the high temperature hydrothermal technique provide ability to grow high quality single crystals at relatively low temperatures ($500\text{-}700^\circ\text{C}$ and $1\text{-}3$ kbar).
- Further, our group has been proved that the high temperature hydrothermal technique can be utilized with exceptionally reactive fluids under extreme conditions of temperature and pressure.
- As a significant breakthrough, we recently found that the use of extremely concentrated hydroxides ($30\text{-}40$ M KOH) and fluorides ($20\text{-}30$ M CsF) allow us to solubilize most inert refractory oxides such as ThO_2 , HfO_2 , ZrO_2 , Nb_2O_5 and Ta_2O_5 .
- Use of these methods allowed us not only to explore new phase space rapidly and prepare interesting new materials, but we can also grow high quality bulk single crystals that are large enough to use in real world applications.
- This demonstration mainly concentrated on the high temperature hydrothermal synthesis of single crystals and structure characterization of rare earth niobates and tantalates.

Synthesis and Structure Characterization

Single Crystal Growth



- All the reactions were performed in silver ampoule ($3/8" \times 3"$).
- ~ 400 mg of reactants were loaded into silver ampoule with 0.8 mL of 30 M KOH.
- Ampoules were weld-sealed and loaded into a 718 Inconel autoclave with a 75% fill of DI water to serve as the desired counter-pressure.
- The autoclave was affixed with ceramic band heaters and heated to a constant temperature of 700°C for a duration of $1\text{-}2$ weeks at ~ 650 bar for $1\text{-}2$ weeks.



Single Crystal Characterization

Bruker D8 single crystal diffractometer equipped with Incoatec Mo K α micro focus source and Photon 100 CMOS detector with Mo K α ($\lambda = 0.71073 \text{ \AA}$) was used to characterize the single crystal structure.

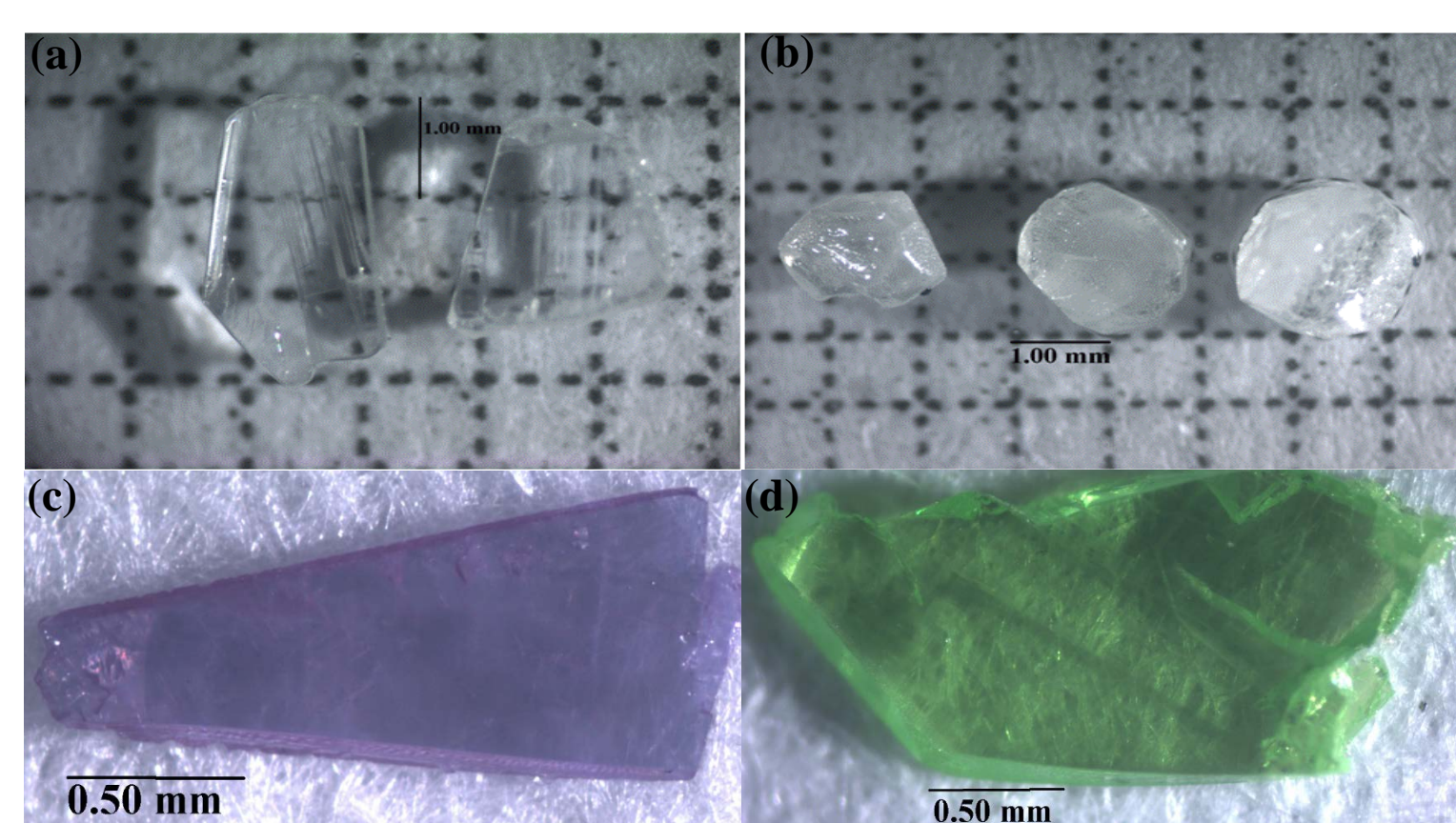


Figure 1. Hydrothermally grown LnNbO_4 . (a) GdNbO_4 , (b) LaNbO_4 , (c) NdNbO_4 and (d) PrNbO_4 .

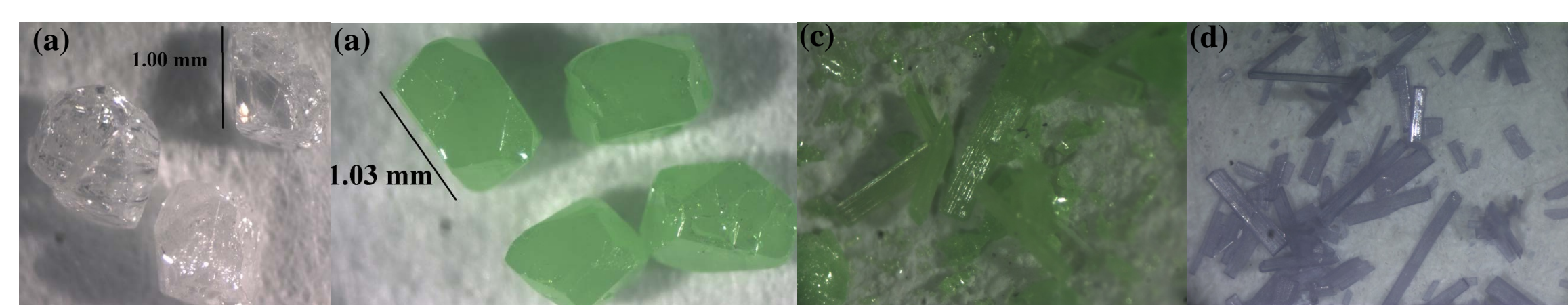


Figure 1. Hydrothermally grown lanthanide tantalates. (a) $\text{La}_2\text{TaO}_5(\text{OH})$, (b) $\text{Pr}_2\text{TaO}_5(\text{OH})$, (c) $\text{Pr}_2\text{Ta}_2\text{O}_9(\text{OH})$ and (d) $\text{Nd}_3\text{Ta}_2\text{O}_9(\text{OH})$.

Crystal Structure Discussion

Rare Earth Niobates (RENbO_4)

Table 1. Crystallographic data of LuNbO_4 .

| | |
|---|--------------------------------|
| empirical formula | LuNbO_4 |
| formula weight (g/mol) | 331.88 |
| temperature (K) | 300(2) |
| crystal system | monoclinic |
| space group | $C2/c$ (no. 15) |
| a , \AA | 6.9805(6) |
| b , \AA | 10.8271(8) |
| c , \AA | 5.0406(4) |
| β , $^\circ$ | 131.676(3) |
| volume (\AA^3) | 284.54(4) |
| Z , calcd density (Mg/m^3) | 4, 7.747 |
| absorption coefficient (mm^{-1}) | 38.321 |
| $F(000)$ | 576 |
| crystal size (mm) | $0.04 \times 0.02 \times 0.02$ |
| $T_{\text{max}}, T_{\text{min}}$ | 1.0000, 0.7062 |
| Θ range for data | $3.76\text{-}26.47$ |
| reflections collected/unique/observed | 1139/297/287 |
| data/restraints/parameters | 297/0/30 |
| goodness-of-fit on F^2 | 1.176 |
| R_1, wR_2 ($I \geq 2\sigma(I)$) | 0.0178, 0.0489 |
| R_1, wR_2 (all data) | 0.0189, 0.0495 |
| extinction coefficient | 0.0051(4) |

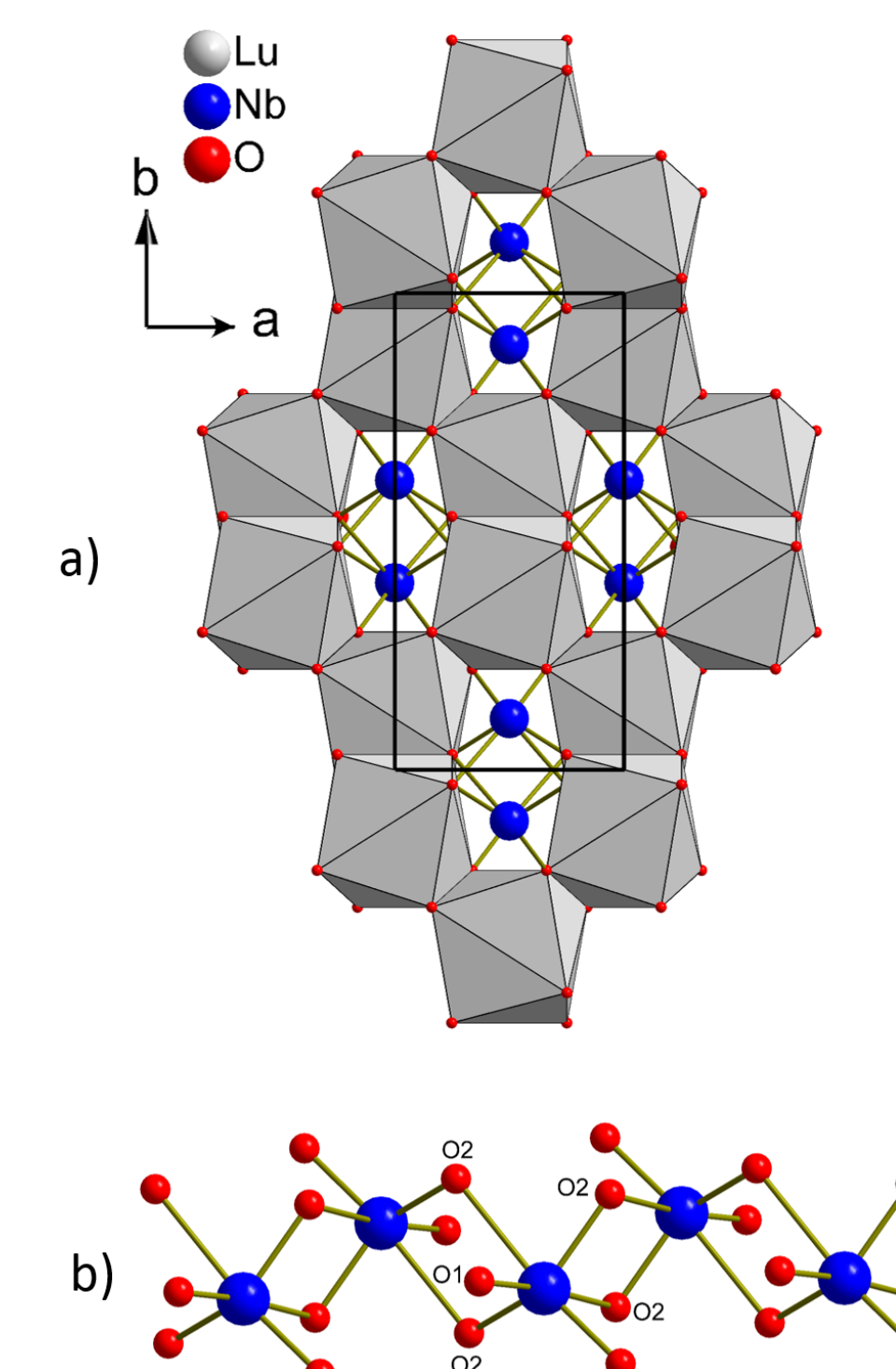


Figure 3. Fergusonite structure type of the rare earth niobates: (a) the framework of edge-sharing LuO_6 units encapsulating chains of NbO_6 units viewed along $[001]$; (b) propagation of the NbO_6 units along $[001]$ through shared $\text{O}(2)$ edges.

$\text{Ln}_2\text{TaO}_5(\text{OH})$ Series

Table 2. Crystallographic data of $\text{Ln}_2\text{TaO}_5(\text{OH})$, $\text{Ln} = \text{La}$ and Pr .

| | | |
|----------------------|--------------------------------------|--------------------------------------|
| Empirical formula | $\text{La}_2\text{TaO}_5(\text{OH})$ | $\text{Pr}_2\text{TaO}_5(\text{OH})$ |
| Formula weight | 555.78 | 559.78 |
| Crystal system | Monoclinic | Monoclinic |
| space group | $P2(1)/n$ (No. 14) | $P2(1)/n$ (No. 14) |
| a , \AA | 7.0980(14) | 7.0146(14) |
| b , \AA | 6.8033(14) | 6.7119(14) |
| c , \AA | 10.264(2) | 10.120(2) |
| β , $^\circ$ | 94.34(3) | 94.18(3) |
| V , \AA^3 | 494.23(17) | 475.18(17) |
| Z | 4 | 4 |
| Calculated density | 7.469 | 7.825 |
| Goodness-of-fit | 1.178 | 1.123 |
| R_1/wR_2 | 0.0299/0.0767 | 0.0177/0.0415 |

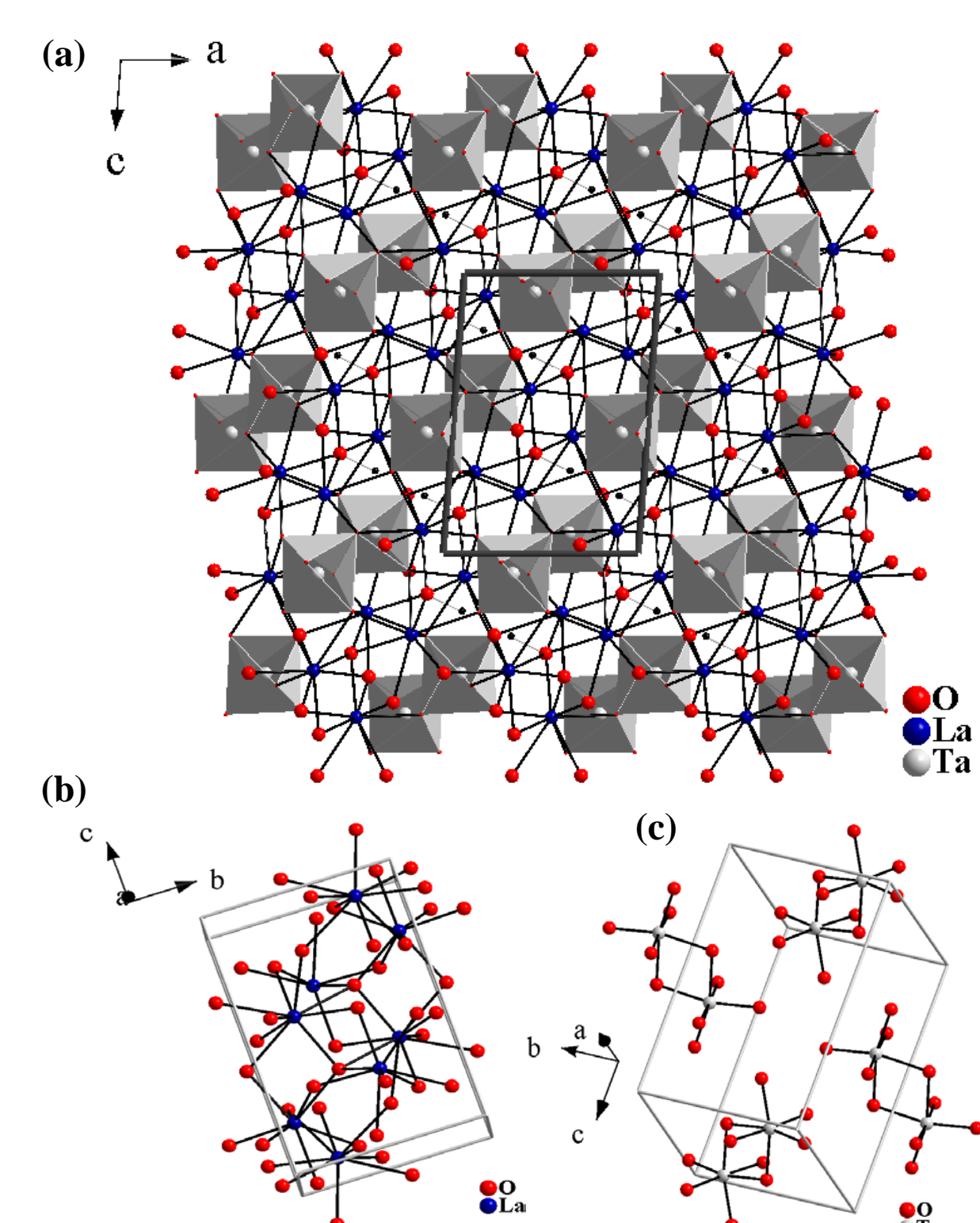


Figure 4. (a) Partial polyhedral view $\text{La}_2\text{TaO}_5(\text{OH})$ showing the connectivity between LaO_6 -polyhedral ($n = 8$ and 9) and TaO_6 -octahedra. (b) The two La sites ($\text{La}(1)\text{O}_6$ and $\text{La}(2)\text{O}_6$) form a 3-D La-O-La lattice. (c) TaO_6 -octahedra forms edge sharing dimers of $[\text{Ta}_2\text{O}_{10}]^{8-}$ units.

$\text{Ln}_3\text{Ta}_2\text{O}_9(\text{OH})$ Series

Table 3. Crystallographic data of $\text{Ln}_3\text{Ta}_2\text{O}_9(\text{OH})$, $\text{Ln} = \text{Pr}$ and Nd .

| | | |
|----------------------|---|---|
| Empirical formula | $\text{Pr}_3\text{Ta}_2\text{O}_9(\text{OH})$ | $\text{Nd}_3\text{Ta}_2\text{O}_9(\text{OH})$ |
| Formula weight | 945.64 | 955.63 |
| Crystal system | Orthorhombic | Orthorhombic |
| space group | Pnmm (No. 58) | Pnmm (No. 58) |
| a , \AA | 19.352(4) | 19.299(4) |
| b , \AA | 5.5764(11) | 5.5533(11) |
| c , \AA | 7.7032(15) | 7.6803(15) |
| V , \AA^3 | 831.3(3) | 823.1(3) |
| Z | 4 | 4 |
| Calculated density | 7.556 | 7.711 |
| Goodness-of-fit | 1.188 | 1.177 |
| R_1/wR_2 | 0.0383/0.0906 | 0.0271/0.0615 |

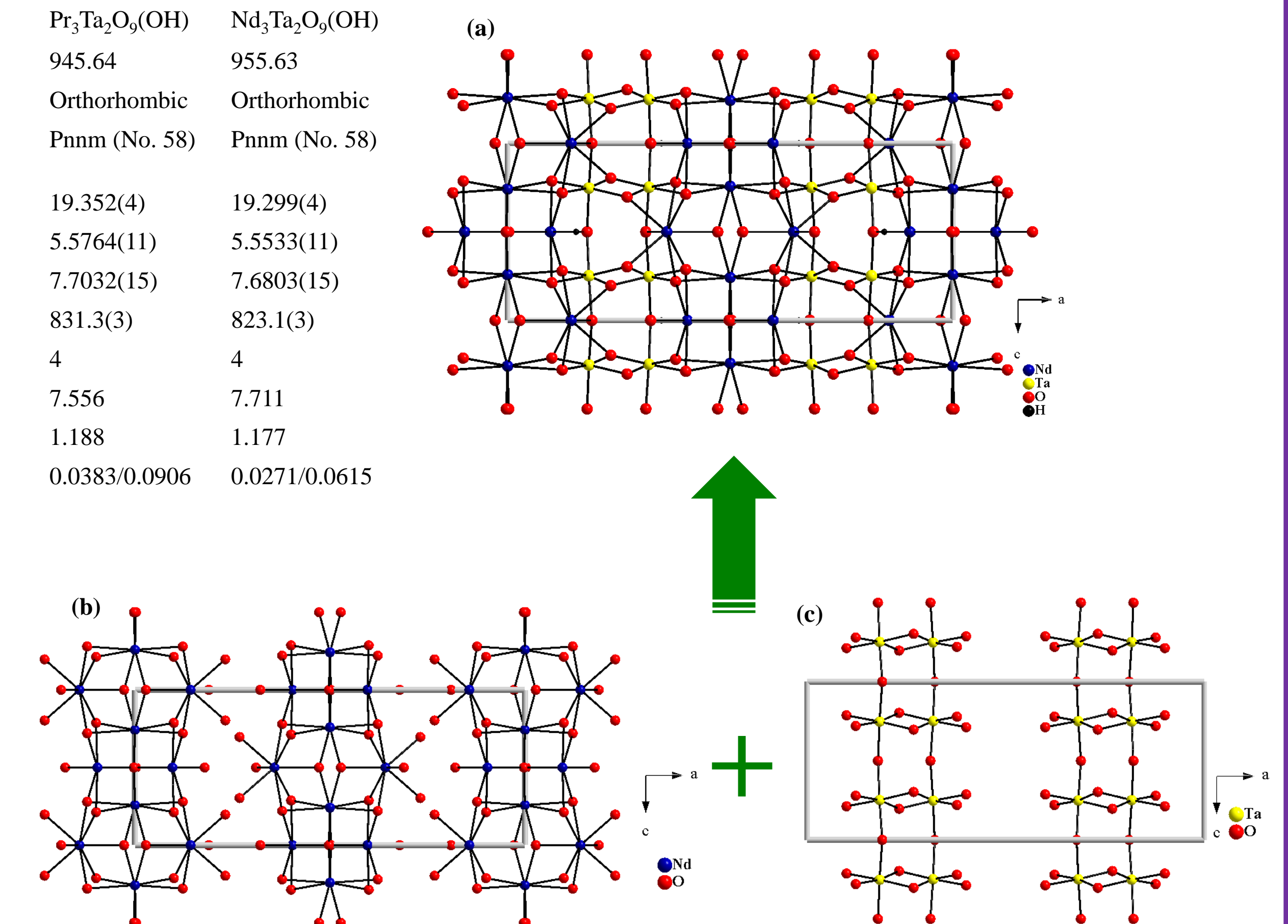


Figure 7. Shows the construction of $\text{Nd}_3\text{Ta}_2\text{O}_9(\text{OH})$ structure. (a) Projected view of $\text{Nd}_3\text{Ta}_2\text{O}_9(\text{OH})$ structure along b -axis. (b) 2-D Nd-O-Nd lattice run parallel to each other along bc -plane. There are three crystallographically distinct Nd sites, $\text{Nd}(1)\text{O}_8$, $\text{Nd}(2)\text{O}_8$, and $\text{Nd}(3)\text{O}_8$. NdO_6 -polyhedral shares edges via oxygen atoms to form the 2-D Nd-O-Nd lattice. (c) Ta-O-Ta chains run along the c -axis. Tantalum forms TaO_6 -octahedra and these octahedra share edges to form $[\text{Ta}_2\text{O}_{10}]^{10-}$ dimeric units and these dimeric units corner shared with two other dimeric unit along the c -axis to form infinite chains. Two 2-D Nd-O-Nd sheets are interconnected by Ta-O-Ta chains along the a -axis to provide a 3-D nature to $\text{Nd}_3\text{Ta}_2\text{O}_9(\text{OH})$ structure.

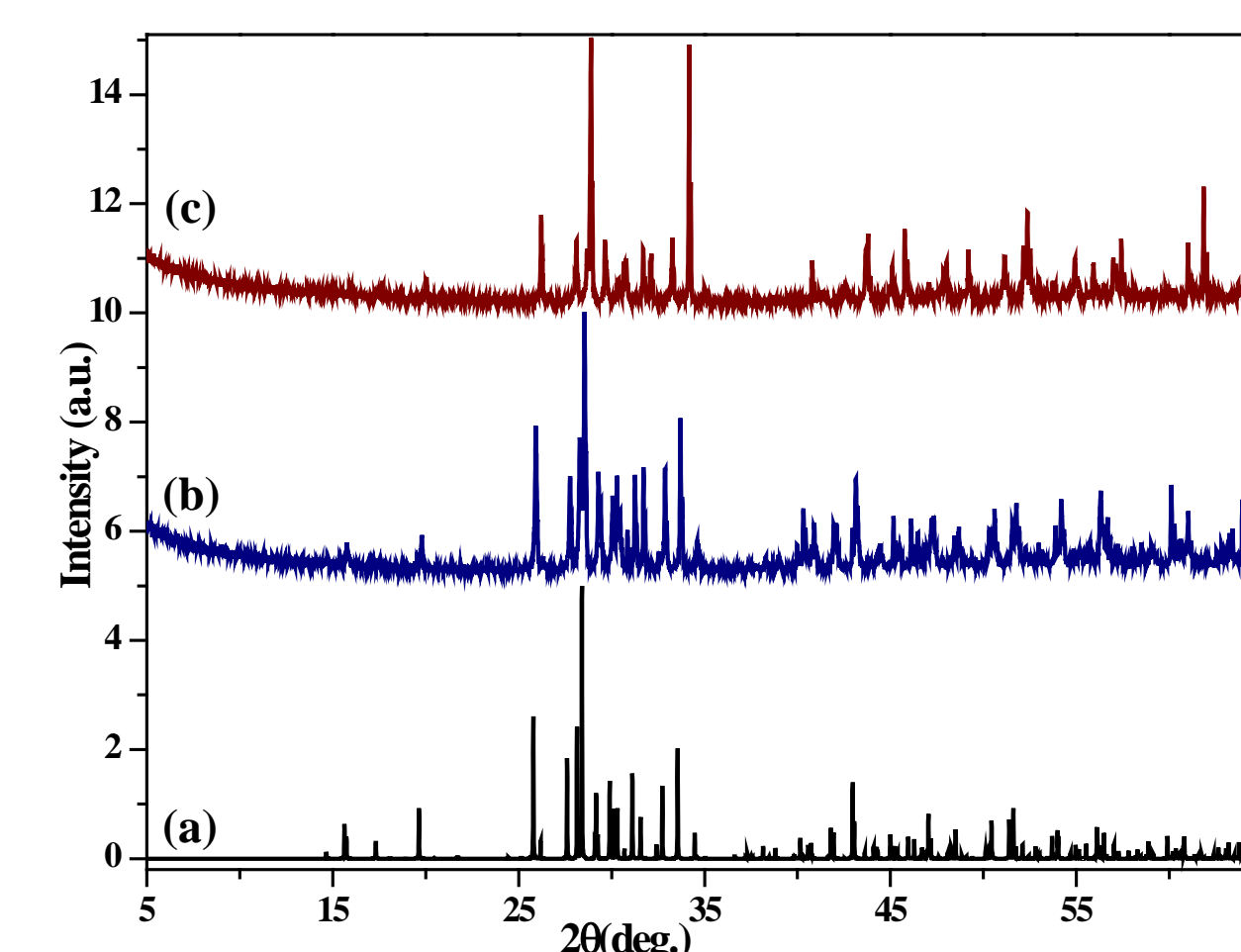


Figure 5. PXRD patterns of (a) calculated $\text{La}_2\text{TaO}_5(\text{OH})$; (b) observed $\text{La}_2\text{TaO}_5(\text{OH})$; (c) observed $\text{Pr}_2\text{TaO}_5(\text{OH})$.

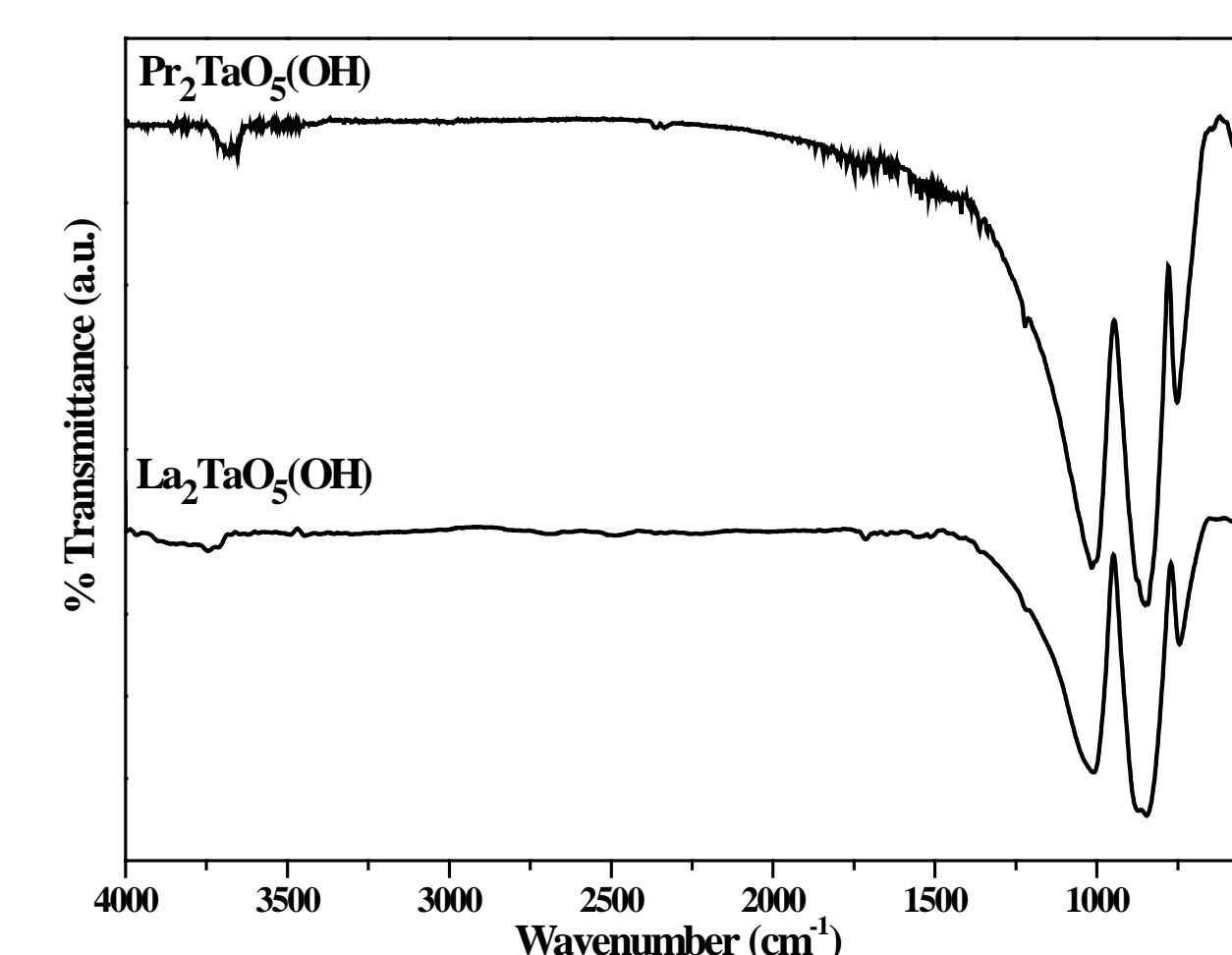


Figure 6. FTIR of $\text{La}_2\text{TaO}_5(\text{OH})$ and $\text{Pr}_2\text{TaO}_5(\text{OH})$. The peaks around 3600 cm^{-1} confirm the presence of hydroxide group in the structure.

Conclusion

- In this study we demonstrate that the rare earth niobates and tantalates can be grown as large high quality single crystals by employing the hydrothermal technique at extreme temperatures ($650\text{-}700^\circ\text{C}$) using extreme alkali hydroxide solutions (30 M KOH).
- This technique often resulted $1\text{-}3$ mm size crystals with good quality for potential of optical applications.
- Further we confirm that the hydrothermal technique can be used to separate low temperature RENbO_4 ($\text{RE} = \text{Y, La-Lu}$) phase which crystallize in the space group of $C2/c$ ($<700^\circ\text{C}$) from its high temperature tetragonal phase ($>800^\circ\text{C}$).
- The preparation of lanthanide doped single crystals of the YNbO_4 phase was also achieved, and the study of their optical properties is ongoing.
- Additionally, use of similar technique with tantalum oxide (Ta_2O_5) with rare earth oxide was also fruitful resulting two series of novel rare earth tantalate structures, $\text{Ln}_2\text{TaO}_5(\text{OH})$ and $\text{Ln}_3\text{Ta}_2\text{O}_9(\text{OH})$.
- The compositions and structural differences in $\text{Ln}_2\text{TaO}_5(\text{OH})$ and $\text{Ln}_3\text{Ta}_2\text{O}_9(\text{OH})$ provide an excellent example of the ability of Ta^{5+} to form different RE-O-Ta oxide lattices.
- Furthermore, the synthesis of new rare earth tantalates explore the possibility of synthesizing new materials targeting photocatalysts, host lattices for phosphors, and ion conductors.
- Finally, future work will test to whether the hydrothermal crystal growth concepts demonstrated in this study can be extended to other refractory oxides with high temperature phase transitions, including ferroelectric or ferromagnetic materials.

Acknowledgements

We are indebted to the Department of Energy Basic Energy Sciences Award Number DE-SC0014271 for support of this work. Purchase of the Bruker single crystal diffractometer was enabled by an internal grant from the office of the Clemson University Vice President for Research.

References

- Hwu, S.-J. Chem. Mater. 1998, 10, 2846-2859.
- Queen, W. L.; Hwu, S.-J.; Wang, L. Angew. Chem. Int. Ed. 2007, 46, 5344-5347.
- Bujoli, B.; Pena, O.; Palvadeau, P.; Bideau, J.L.; Payen, C.; Rouxel, J. Chem. Mater., 1993, 5, 583-587.
- Chung, E.M.L.; Lees, M.R.; McIntyre, G.J.; Wilkinson, C.; Balakrishnan, G.; Hague, J.P.; Visser, D.; McK Paul, D. J. Phys. Condens. Matter, 2004, 16, 7837-7852.
- Tung, L. D.; Lees, M. R.; Balakrishnan, G.; Paul, D. M. Phys. Rev. B. 2007, 75, 104404.